Energy dissipation of the friction sliding isolation structure with MoS_2 as the lubricating material

Jiangle Li[1,2,*], Sheliang Wang[1], Li Gao[1], Yanzhou Hao[1,2], Meng Zhan[1]

1. School of civil Engineering, Xi'an University of Architecture and Technology, 13 Yanta Road, Beilin District, Xi'an 710055, China

2. College of Urban, Henan University of Urban Constuction, Longxiang Street, Xincheng District, Pingdingshan 467036, China

30080206@hncj.edu.cn

ABSTRACT. *Considering the importance of friction coefficient in bearing performance and the good properties of MoS_2, this paper designs an innovative friction sliding isolation bearing with MoS_2 as the lubricating material. The relationship between the friction coefficient and the compressive stress was determined by fitting the results of a loading test, and the feasibility of the material was proved through a shaking table test on a five-layer concrete frame model. Based on the energy dissipation theory, the seismic behavior of the proposed friction sliding isolation structure was simulated on MATLAB/Simulink. The simulation results show that the entire structure had little displacement, despite the slight slippage of the isolation layer, under the simulated earthquake wave. The energy response at different friction coefficients shows that the total seismic energy input of the system increased with the friction coefficient. The change of the total seismic input was not obvious when the friction was up to 0.15. The research findings shed new light on the application of isolation devices in practical engineering.*

RÉSUMÉ. *Compte tenu de l'importance du coefficient de frottement dans les performances de roulement et des bonnes propriétés du MoS_2, ce papier conçoit un roulement innovant à isolement par glissement de friction avec du MoS_2 comme matériau lubrifiant. La relation entre le coefficient de frottement et la contrainte de compression a été déterminée en adaptant les résultats d'un test de chargement, et la faisabilité de la matière a été prouvée par un test de table à secousses sur un modèle de structure en béton à cinq couches. Sur la base de la théorie de la dissipation d'énergie, le comportement sismique de la structure d'isolation par glissement de friction proposée a été simulé sur MATLAB / Simulink. Les résultats de la simulation montrent que la structure entière avait peu de déplacement, malgré le léger glissement de la couche d'isolation, sous la vague de tremblement de terre simulée. La réponse énergétique à différents coefficients de frottement montre que l'apport d'énergie sismique totale du système a augmenté avec le coefficient de frottement. Le changement de l'apport sismique total n'était pas évident lorsque le frottement atteignait 0,15. Les résultats*

de la recherche ont permis de mieux comprendre l'application des dispositifs d'isolation en ingénierie pratique.

KEYWORDS: *friction sliding isolation, energy dissipation, MoS_2, seismic response, shaking table test.*

MOTS-CLÉS: *isolation par glissement de friction, dissipation d'énergie, MoS_2, réponse sismique, test de la table à secousses.*

DOI:10.3166/ACSM.42.303-316 © 2018 Lavoisier

1. Introduction

Vibration isolation is a safe, economic and convenient damping technology capable of preventing sympathetic vibration, extending the natural vibration period of structures, and suppressing random seismic excitations. One of the most promising isolation techniques is the friction sliding isolation system, which dissipates the seismic energy through the friction of structure sliding in earthquakes.

Over the years, the friction sliding isolation system has developed from a simple pure friction structure to a complex structural system with a simple but effective isolation solution. There many types of friction sliding isolation systems, namely, pure friction sliding isolation system (PF) (Liu *et al*., 2008; Ma *et al*., 1982; Existing, 2010), sliding isolation structure with limiting device (Xiong *et al*., 2003), resilient friction base isolation system (R-FBI) (Hong and Feng, 1993; Mostaghel and Khodaverdian, 1987; Jankowski and Mahmoud, 2015; Su and Ahmadi, 1992), series isolation system (Gur and Mishra, 2013), slip-reset friction isolation system (Lu *et al*., 2007) and friction pendulum isolation system (FPS) (Ponzo *et al*., 2017; Zayas *et al*., 2000; Mokha *et al*., 1991).

In 1999, Chinese academician Zhou *et al*. (1999) systematically explored the low-cost friction sliding isolation structure of Teflon pate and steel damper through a shaking table test. However, there is no report on the damping dissipation energy and the structure simulation of this type of friction sliding isolation structure.

2. Design and loading test of sliding isolation bearing

In this paper, a new sliding isolation bearing is designed (Figure 1) with MoS_2 solid powder as the lubricating material. On the microscale, MoS_2 consists of numerous hexagonal grids of S-Mo-S. The strong polar bond of S-Mo is hard to break, while the weak molecular bond of S-S is easy to damage. A small shear stress is enough to cause the sliding between different layers of the molecular structure. Thus, MoS_2 enjoys good lubricating properties on the macroscale, which are useful in isolation systems. In the designed bearing, the upper plate, the lower plate and the slider were all sprayed with MoS_2.

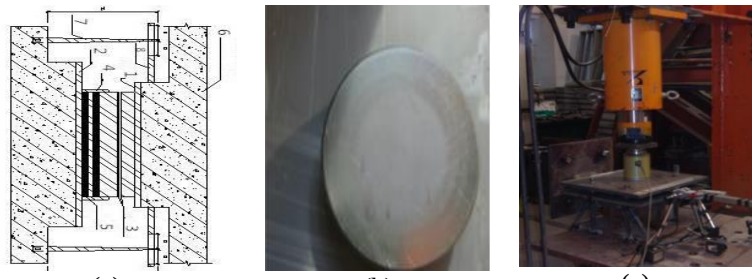

(a) (b) (c)

Figure 1. Design and loading test of sliding isolation bearing ((a) Bearing structure (1. Upper plate; 2. Lower plate; 3. MoS_2 layer; 4. Rubber; 6. Base beam; 7. Displacement controller; 8. Guide plate); (b)Slider; (c) Loading device)

Then, the friction behavior of the designed friction sliding bearing was tested through a loading test at the stresses of 35t, 45t, 55t, 65t and 75t. The stresses were applied by the loading device in Figure 1(c). Each stress was applied twice to determine the accurate relationship between the restoring force and the displacement (Figure 3).

Table 1. The test conditions

Condition	Sample	Lubricating material	Stress (t)
1	Two identical sliders, respectively for the first and second loading at each stress	MoS_2	35
2			45
3			55
4			65
5			75

Based on the test data, the relationship between the friction coefficient and the compressive stress (Figure 4) can be fitted as:

$$\mu = 0.043 + 0.04804e^{-\frac{\sigma}{18.84046}} \tag{1}$$

The fitted values of the friction coefficient were then contrasted against the test values (Figure 2).

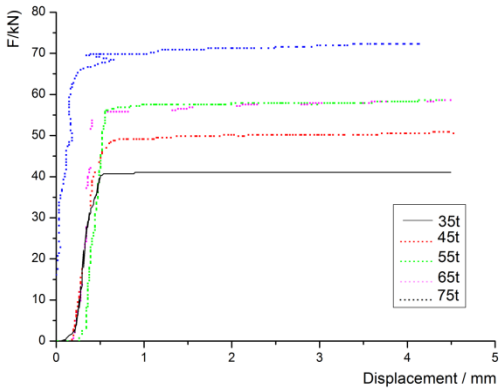

Figure 2. Relationship between the restoring force and the displacement

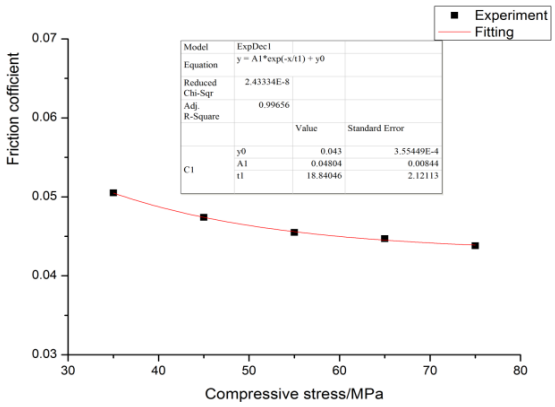

Figure 3. Relationship between friction coefficient and compressive stress

Table 2. Comparison between the fitted values and test values of the friction coefficient

Compressive stress /t	Test value	Fitted value	Error rate/%
35	0.0505	0.050496	0
45	0.0474	0.04740	0.1
55	0.0455	0.04559	0.3
65	0.0447	0.044525	0.2
75	0.0438	0.04389	0.2

It can be seen from the above that the restoring force of the bearing accords with the Coulomb model of friction, indicating that the design is reasonable. In addition, with an error rate no greater than 0.3, the friction coefficient can be used for our bearing.

3. Damping energy dissipation

To verify the feasibility of using MoS_2 as the coating material of our bearing, a shaking table test was carried out to simulate the damping effect and slippage of the new sliding isolation bearing at different seismic intensities.

3.1. Five-layer frame model

For the shaking table test, the author designed a five-layer concrete frame model of the scale of 1:5. As shown in Figure 5, nine sliding isolation bearings were arranged at the bottom of each column; on the edge of the structural floor, slotted steel slide plates were embedded to limit the displacement of the conical rods; the seismic isolation device was installed between the bottom plate and the base plate. Together, these components formed a seismic isolation layer.

(a) (b) (c)

Figure 5. Five-layer frame model ((a) Installation of isolation bearings;(b) Embedment of slotted steel slide plates; (c) The frame model)

3.2. Test conditions

The shaking table test was conducted on a 4m×4m shaking table at the Key Lab of Structure and Earthquake Resistance, Xi'an University of Architecture and Technology. Three seismic waves with different seismic intensities and site conditions were selected to test the damping effect and slippage law, including El Centro wave, Tianjin wave and Lanzhou wave. The original signals are displayed in Figure 6 below, and the peak ground acceleration (PGA) of the three waves are 197gal, 394gal and 591gal, respectively. The values were fined tuned for the respective test conditions.

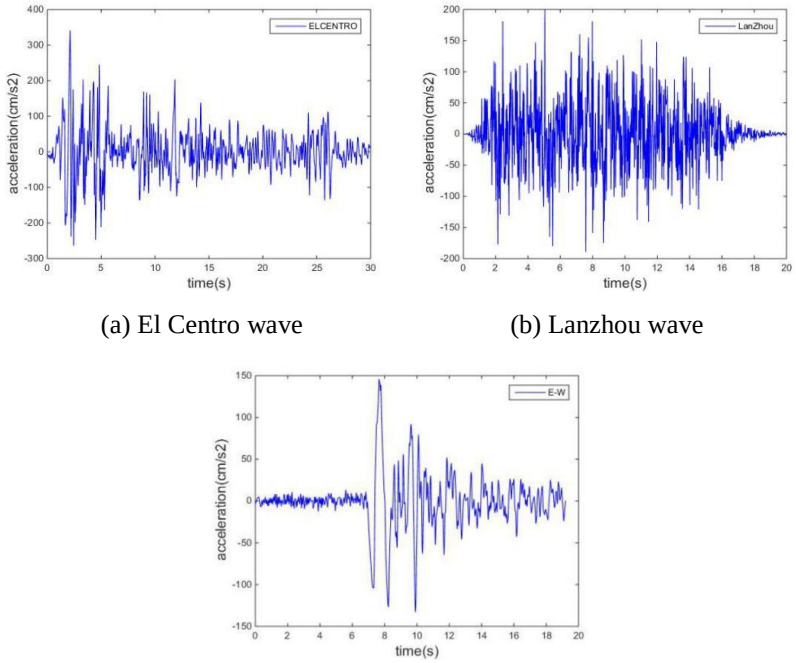

(a) El Centro wave (b) Lanzhou wave

(c) Tianjin wave

Figure 6. Acceleration-time curves

Under the first test condition, a.k.a. the slip limit condition, the base plate was placed on the shaking table and fixed onto the platform via a steel bar (Figure 5(b)). Under the second test condition, a.k.a. the normal test condition, the friction sliding bearings were removed from the frame model (i.e. the isolation system was not used), and the columns and the base plate were fixed by high-strength bolts. The displacement and strain of this condition were collected and compared with those of the first test condition.

3.3. Result comparison

The acceleration responses of each test condition were acquired from white-noise sweeps before and after the earthquake. Then, the transfer functions for the top and bottom of the vibration table before and after vibrations were derived for the two test conditions. On this basis, the author determined the natural frequencies of the test structure in the first three orders before and after the earthquake (Table 3).

Table 3. Natural vibration frequencies in the first three orders (A: Post-earthquake; B: Pre-earthquake)

Test condition	First order frequency/Hz		Second order frequency/Hz		Third order frequency/Hz	
	B	A	B	A	B	A
Slip limit condition	4.94	4.84	7.40	7.44	16.23	14.91
Normal test condition	5.65	4.66	19.59	17.84	26.39	25.83

As shown in Table 3, the first-order natural vibration frequency was greater in normal test condition than in slip limit condition, revealing that the friction sliding bearings can reduce the natural vibration frequency and prolong the natural vibration period of the structural system. After the earthquake, the frequency of the slip limit model decreased slightly, which is much weaker than the frequency decline of the normal test model. This means that the normal test model underwent stiffness attenuation due to the seismic damages, and that the sequence of the test conditions is rational. The slip limit condition should be arranged before the normal test condition. Otherwise, the structural system will be damaged at the beginning of the test.

Figure 7 shows the acceleration-time curve s of the fifth layer at different waves. It is clear that the structural system had a smaller acceleration under the slip limit condition than under the normal test condition.

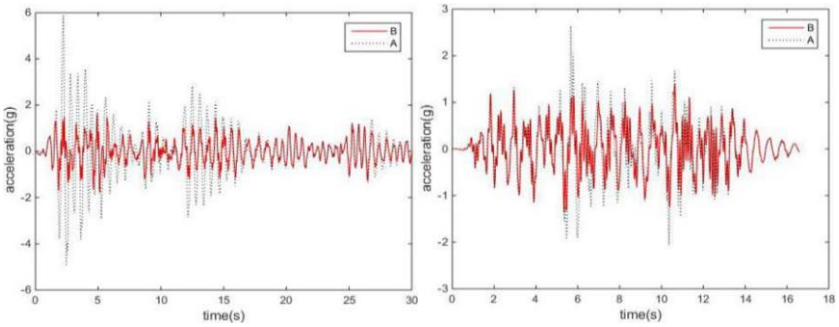

(a) El Centro wave (b) Lanzhou wave

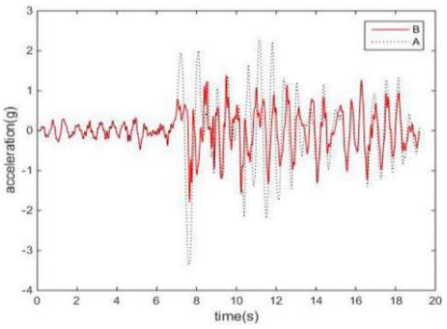

(c) Tianjin wave

Figure 7. Acceleration-time curves of the fifth layer (A: The normal test condition; B: The slip limit condition)

4. Isolation layer energy dissipation

4.1. Theoretical derivation

In the friction sliding isolation system, the structural transformation mainly appears in the isolation layer. Thus, the energy dissipation ability of this layer directly bears on the seismic behavior of the entire structure. This section attempts to disclose the fundamental dissipation ability of the isolation layer based on the energy design. The energy-balance equation of the structure can be derived by integrating the equations of structural motion at any time *t*:

$$\int_0^t \dot{x}^T M\ddot{x}dt + \int_0^t \dot{x}^T C\dot{x}dt + \int_0^t \dot{x}^T Kxdt + \int_0^t \dot{x}^T F(x)dt = -\int_0^t \dot{x}^T M\{I\}\ddot{x}_g dt \qquad (2)$$

Then, the total energy of the seismic input at time *t* can be expressed as:

$$E(t) = -\int_0^t \dot{x}^T M\{I\}\ddot{x}_g dt \qquad (3)$$

The dynamic force of the structure system at time *t* can be expressed as:

$$E_k(t) = \int_0^t \dot{x}^T M\ddot{x}dt \qquad (4)$$

The damping dissipation energy of the structure at time *t* can be expressed as:

$$E_c(t) = \int_0^t \dot{x}^T C\dot{x}dt \qquad (5)$$

The deformation energy of the structure at time *t* can be expressed as:

$$E_e(t) = \int_0^t \dot{x}^T Kxdt \qquad (6)$$

The hysteretic energy of the structure at time *t* can be expressed as:

$$E_d(t) = \int_0^t \dot{x}^T F(x) dt = E_f(t) + E_h(t) \tag{7}$$

where $E_f(t)$ is the friction energy dissipation of the isolation layer at time *t*; $E_h(t)$ is the cumulative plastic deformation energy of the slotted steel slide plate at time *t*; [M], [C] and [K] are the mass matrix, damping matrix and stiffness matrix, respectively; $x = [x_0, x_1, x_2, \cdots, x_n]^T$, $\dot{x} = [\dot{x}_0, \dot{x}_1, \dot{x}_2, \cdots, \dot{x}_n]^T$ and $\ddot{x} = [\ddot{x}_0, \ddot{x}_1, \ddot{x}_2, \cdots, \ddot{x}_n]^T$ are the displacement, the velocity and the accelerated velocity; respectively; {I}is the unit column vector; $F(x)$ is the restoring force vector of the element in the isolation layer.

Equation (2) can be simplified as:

$$E(t) = E_k(t) + E_c(t) + E_e(t) + E_d(t) \tag{8}$$

At the end of the earthquake, the dynamic energy and the deformation energy can be ignored. Then, the energy balance equation of the friction sliding isolation structure can be rewritten as:

$$E(t_0) = E_c(t_0) + E_d(t_0) \tag{9}$$

4.2. Simulink simulation

With the aid of MATLAB/Simulink, the author created the Simulink models of the friction sliding isolation structure and the energy response of the upper part of the structure (Figure 8). The models are discontinuous Coulomb friction model, in which the static friction coefficient is equal to the dynamic friction coefficient.

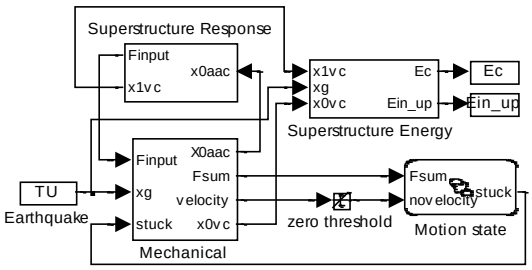

(a) Simulink model of the friction sliding isolation structure

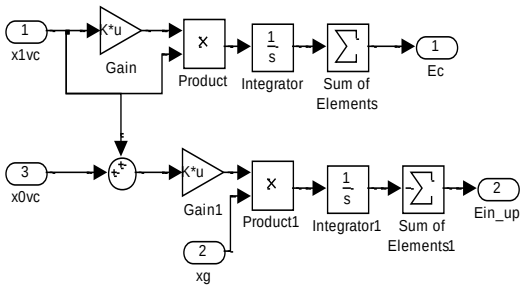

(b) Simulink model of the energy response of the upper part of the structure

Figure 8. Simulink models

The energy-oriented seismic assessment mainly focuses on three issues: the total seismic energy input of the structure, the energy dissipation property of each part of the structure, and the assessment method. The first two issues are the top priority.

At the end of the earthquake, the dynamic energy and the deformation energy are almost zero. In this case, the energy input of the structure is made up of the damping dissipation energy of the structure and the hysteretic energy of the isolation layer. The three energies can be calculated by equations (3), (5) and (9) and simulated by Simulink. For simplicity, the evaluation indices can be defined as:

Damping dissipation ratio of the structure:

$$\lambda_c = \frac{E_c}{E_{in}} \tag{9}$$

Hysteretic energy ratio of the isolation layer:

$$\lambda_d = \frac{E_d}{E_{in}} \tag{10}$$

Energy isolation rate:

$$\eta = \frac{E_{ink} - E_{ing}}{E_{ink}} \times 100\% \tag{11}$$

where E_{in} is the total energy of the structure at the end of the earthquake; E_c is the damping dissipation of the structure at the end of the earthquake; E_d is the hysteretic energy of the isolation layer at the end of the earthquake; E_{ink} is the total seismic input of the structure; E_{ing} is the total energy input of the structure under the slip-limit condition. The value of the hysteretic energy ratio of the isolation layer λ_d is positively correlated with the energy dissipation ability and the isolation effect of the damper. For an isolation device with sufficient dissipation ability, its λ_d value must

be greater than the damping dissipation ratio of the structure. In addition, the energy isolation rate η is positively correlated with the overall isolation performance.

4.3. Results comparison

Based on the scale of the test model, the displacement of the isolation layer can be derived from that of the friction sliding isolation structure. Table 4 compares the simulated and test values of isolation layer displacement, aiming to validate the simulation process.

Table 4. Simulated and test displacements of the isolation layer (mm)

Intensity	El Centro wave		
	Test value	Derived value	Simulated value
0.2g	5.84	29.2	24.64
0.4g	24.29	121.45	115.2
0.6g	40.85	204.25	195.62
Intensity	Tianjin wave		
	Test value	Derived value	Simulated value
0.2g	25.45	127.25	128.73
0.4g	44.84	224.2	216.33
0.6g	80	400	395.17
Intensity	Lanzhou wave		
	Test value	Derived value	Simulated value
0.2g	1.88	9.4	7.94
0.4g	9.37	46.85	39.88
0.6g	42.31	211.55	207.7

It can be seen from Table 4 that the displacement derived for the isolation layer was close to the simulated value. The error is so small that the MATLAB/Simulink is an acceptable tool for seismic response analysis of the friction sliding isolation structure under strong motions. The El Centro wave was selected for the subsequent discussion.

4.4. Effect of friction coefficient on the friction sliding isolation structure

The El Centro wave was selected as the seismic wave when the structure is in a pure slip state. The corresponding acceleration peaks are 0.2g, 0.4g and 0.6g. If the

friction coefficient is infinite, it means the structure is seismic resistant. Table 5 and Figure 9 provide the energy level and evaluation indices in various parts of the structure as well as the total seismic input of the system at different frictions.

Table 5. The energy level and evaluation indices at 0.4g (kJ)

Friction coefficient	E_{in}	E_c	λ_c	E_d	λ_d	E_c+E_d	η/%
0.03	321.51	31.93	0.10	288.18	0.90	320.11	52.21
0.07	517.03	100.35	0.19	413.34	0.80	513.68	23.14
0.1	579.19	149.52	0.26	426.70	0.74	576.22	13.90
0.15	629.99	240.57	0.38	386.36	0.61	626.93	6.35
0.2	655.40	299.76	0.46	352.36	0.54	652.12	2.58
0.25	647.01	339.89	0.53	303.57	0.47	643.46	3.82
0.3	646.61	392.56	0.61	250.40	0.39	642.95	3.88
∞	672.73	668.55	0.99	0.00	0.00	668.55	0.00

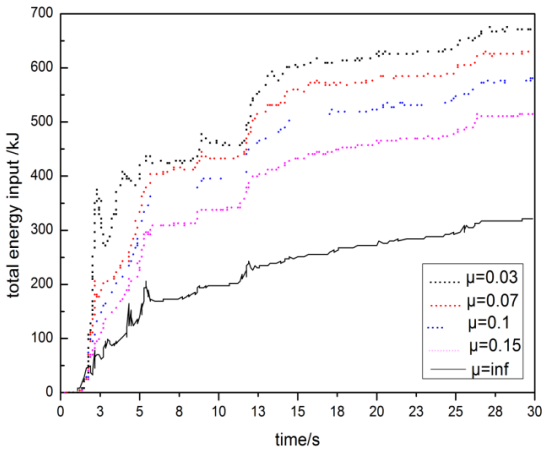

Figure 9. The total seismic input of the structure at 0.4g

As shown in the above table and figure, the total seismic input of the structure increased with the friction coefficient. The change of the total seismic input was not obvious when the friction was up to 0.15. When the friction coefficient increased from 0.03 to 0.15, the damping dissipation energy E_c and the corresponding damping dissipation ratio λ_c underwent a gradual decline, while the hysteretic energy of the isolation layer E_d showed a complex variation pattern.

5. Conclusions

This paper puts forward a new sliding isolation bearing with MoS_2 as the lubricating material. The material was proved to have a stable frictional performance through a loading test. Then, the relationship between the friction coefficient and the compressive stress was determined by fitting the test results. It is found that the restoring force of the isolation layer accords with the Coulomb model of friction, which confirms the validity of our bearing.

Next, a five-layer frame model was design to measure the damping effect and slippage of the friction sliding isolation structure at different seismic intensities through a shaking table test. The test results show that the isolation technology reduced the natural frequency and extended the natural vibration period of the structure. Through MATLAB/Simulink simulations, it is learned that the entire structure had little displacement, despite the slight slippage of the isolation layer, under the simulated earthquake wave.

The energy response at different friction coefficients shows that the total seismic energy input of the system increased with the friction coefficient. The change of the total seismic input was not obvious when the friction was up to 0.15. When the friction coefficient increased from 0.03 to 0.15, the damping dissipation energy and the corresponding damping dissipation ratio underwent a gradual decline, while the hysteretic energy of the isolation layer E_d showed a complex variation pattern.

Acknowledgments

Thanks for the natural sciences foundation (51178388), the SHAN XI province industrial project (2013K07-07, 2014K06-34) and the SHAN XI province education department natural project(2013JK0612,14JK1420).

Basic Scientific Research of Central Colleges (No. 310841171001), Shaanxi Province Postdoctoral Research Project (No. 332100160021), Natural Science Research Projects of Shaanxi (2017JQ5061).

References

Existing M. Y. H. (2010). Codes on earthquake design with and without seismic devices and tabulated data. *Earthquake Resistant Buildings*, pp. 51-141. http://doi.org/10.1007/978-3-540-93818-7_2

Gur S., Mishra S. K. (2013). Multi-objective stochastic-structural-optimization of shape-memory-alloy assisted pure-friction bearing for isolating building against random earthquakes. *Soil Dynamics & Earthquake Engineering*, Vol. 54, pp. 1-16. http://doi.org/10.1016/j.soildyn.2013.07.013

Hong F., Feng Q. M. (1993). Analysis of earthquake reliability for structures with resilience-friction base isolation system. *Earthquake Engineering and Engineering Vibration*, Vol. 13, No. 4, pp. 81-88.

Jankowski R., Mahmoud S. (2015). Pounding between buildings. *Earthquake-Induced Structural Pounding*, pp. 35-71. http://doi.org/10.1007/978-3-319-16324-6_3

Liu H. Q., Wang X. Q., Wang J. L. (2008). Catastrophic seismic response of isolated structure based on laminated rubber bearings. *Journal of Earthquake Engineering and Engineering Vibration*, Vol. 28, No. 2, pp. 158-164.

Lu L. H., Xu Z. D., Shi C. F. (2007). Research status and development of structural sliding isolation technology. *Journal of Disaster Prevention and Mitigation Engineering*, Vol. 27, pp. 243-246.

Ma G. W., Hao H., Lu Y. (2010). Modelling damage potential of high‐frequency ground motions. *Earthquake Engineering & Structural Dynamics*, Vol. 32, No. 10, pp. 1483-1503. https://doi.org/10.1002/eqe.282

Mokha A., Constantinou M. C., Reinhom A. M., Zayas V. A. (1991). Experimental study of friction pendulum isolation system. *Journal of Structural Engineering*, Vol. 117, No. 6, pp. 1201-1218. http://doi.org/10.1061/(ASCE)0733-9445(1991)117:4(1201)

Mostaghel N., Khodaverdian M. (1987). Dynamics of resilient-friction base isolator (R-FBI). *Earthquake Engineering and Structural Dynamics*, Vol. 15, No. 3, pp. 379-390. http://doi.org/10.1002/eqe.4290150307

Ponzo F. C., Cesare A. D., Leccese G., Nigro D. (2017). Shake table testing on restoring capability of double concave friction pendulum seismic isolation systems. *Earthquake Engineering & Structural Dynamics*, Vol. 46, No. 6, pp. 2337-2353. https://doi.org/10.1002/eqe.2907

Su L., Ahmadi G. (1992). Probabilistic responses of base-isolated structures to El Centro 1940 and Mexico City 1985 earthquakes. *Engineering Structures*, Vol. 14, No. 4, pp. 217-230. http://doi.org/10.1016/0141-0296(92)90010-N

Xiong Z. M., Yu M. H., Wang Q. M. M., Feng D. G., Shui H. X., Shui G. F. (2003). Theoretical study on design and application on sliding base isolation structure. *Journal of Vibration and Shock*, Vol. 22, No. 3, pp. 50-54. http://doi.org/10.3969/j.issn.1000-3835.2003.03.015

Zayas V., Low S., Mahin S. A. (1990). A simple pendulum technique for achieving seismic isolation. *Earthquake Spectra*, Vol. 6, pp. 317-333. http://doi.org/10.1193/1.1585573

Zhou X. Y., Han M., Zeng D. M., Ma D. H. (1999). Calculation method of lateral stiffness of combined rubber bearing and serial system of bearing with columns. *Earthquake Engineering and Engineering Vibration*, Vol. 19, No. 4, pp. 67-75. http://doi.org/10.1016/1359-0197(89)90099-4